Journal of Fractional Calculus and Applications
Vol. 12(3). No. 18, pp. 1-16
1st. Inter. E-Conf. in Math. Sciences and Fractional Calculus(ICMSFC Feb 2021).
ISSN: 2090-5858.
http://math-frac.org/Journals/JFCA/

THERMAL DIFFUSION AND RADIATION AFFECT THE FREE CONVECTION FLOW OF UNSTABLE MAGNETOHYDRODYNAMIC PAST AN IMPULSIVELY MOVING PLATE WITH RAMPED WALL TEMPERATURE AND RAMPED WALL CONCENTRATION

L. RAMA MOHAN REDDY

Abstract. The present work investigated analytically the influence of thermal diffusion and radiation on unsteady MHD, free connective incompressible flow of viscous, electrically conducting fluid past an impulsively moving isothermal porous plate and for the case of ramped wall temperature and ramped wall concentration. The non-dimensional governing equations are solved in closed form by using Laplace transform method. Exact solutions are obtained for velocity, concentration and temperature. With the help of those expressions - Skin friction, Sherwood and Nusselt numbers are derived. Various physical parameters effect on the above flow equations are studied numerically with the assistance of graphs and tables.

1. Introduction:

Recently Heat transport is one among the weather of natural convection where the fluid motion doesn't generate by external source (like a lover, pump, suction device, etc.) but it generates with density differences within the fluid thanks to temperature gradients. In free convection, fluid surrounding the warmth source receives the warmth and it becomes less dense and rises.

Sahoo [1] studied effects of partial slip, Joule heating and viscous dissipation on Von Karman flow and warmth transfer of an electrically conducting non-Newtonian fluid. Raju et al [2] studied MHD convective flow through porous medium during a horizontal channel with insulated and impermeable bottom wall up the presence of viscous dissipation and Joule heating. S. Siddiqa, S. Asghar, and M. A. Hossain, et al. [3] studied natural convection flow over an inclined flat plate with internal heat generation and variable viscosity. M. S. Alam, M. A. Sattar and M. M. Rahman, et

Key words and phrases. Free convection flow, Magnetohydrodynamic, ramped wall temperature and ramped wall concentration, thermal diffusion and radiation.
Submitted Nov. 13, 2020.

al. [4] investigated effects of variable suction and Thermophoresis on steady MHD combined free-forced convective heat and mass transfer flow over a semi-infinite permeable inclined plate within the presence of thermal radiation. Das SS, Das JK, Satapathy A, Panda JP et al. [5] investigated mass transfer effects on MHD flow and warmth transfer past a vertical porous plate through a porous medium under oscillatory suction and warmth source. Ghosh SK, O.A. Beg et al [6] studied theoretical analysis of radiative effects on transient free convection heat transfer past a hot surface in porous media. Azzam GEA [7] analyzed radiation effects on the MHD mixed free forced convective flow past a semi-infinite moving vertical plate for top temperature differences. Bestman AR [8] studied free convection heat transfer to steady radiating non-Newtonian MHD flow past a vertical porous plate. Mbeledogu, I.U, Amakiri, A.R.C and Ogulu A et al. [9] studied unsteady MHD free convection flow of a compressible fluid past a moving vertical plate within the presence of radiative heat transfer. C. Y. Cheng [10] analyzed Soret and Dufour effects on heat and mass transfer by natural convection from a vertical frustum during a fluid - saturated porous medium with variable wall temperature and concentration. Singha, K.G., Deka, P.K [11] considered skin-friction for unsteady free convection MHD flow between two heated vertical parallel plates. C.H. Chen, Yunlin, Taiwan et al. [12] studied heat and mass transfer in MHD flow by natural convection from a semipermeable, inclined surface with variable wall temperature and concentration.

2. Formulation of the Problem:

Consider flow of a viscous incompressible electrically conducting fluid past an infinite vertical plate embedded in a porous medium. $x^{'}$ -axis is taken along the plate in the upward direction and $y^{'}$ -axis normal to plane of the plate in the fluid. The fluid is permeated orm transverse magnetic field B_0applied parallel to by a unif $y^{'}$ -axis. Initially, at time $t \leq 0$, both the fluid and plate are at rest and at uniform temperature T_∞ and uniform concentration C_∞At time $t > 0$, the plate starts moving along $x^{'}$ direction with uniform velocity U_0 , temperature and concentration of the plate is raised or lowered to $T_\infty + (T_w - T_\infty)t/t_0$,$C_\infty + (C_w - C_\infty)t/t_0$,when $t \leq t_0$, and thereafter, for $t > t_0$, is maintained at uniform temperatureT_w and uniform concentration C_w Since plate is of infinite extent along $X^{'}$ and $Z^{'}$directions and is electrically non-conducting all physical quantities, except pressure, are functions of $y^{'}$ and t only.

It is assumed that induced magnetic field produced by the fluid motion is negligible in comparison to the applied one so that we consider magnetic field $\overrightarrow{B} \equiv (0, B_0, 0)$. This assumption is justified because magnetic Reynolds number is very small for metallic liquids and partially ionized fluids [31]. Also no external electric field is applied so the effect of polarization of fluid is negligible [31], so we assume $\overrightarrow{E} \equiv (0, 0, 0)$.

Taking into account the assumptions made above, the governing equations for laminar natural convection flow of a viscous incompressible electrically conducting fluid past a vertical plate in a uniform porous medium, under Boussinesq approximation, reduce to

$$\frac{\partial u^*}{\partial t^*} = \upsilon \frac{\partial^2 u^*}{\partial y'^2} + g\beta\left(T^* - T_\infty^*\right) + g\beta^*\left(C^* - C_\infty^*\right) - \sigma\frac{B_0^2}{\rho}u^* - \frac{\upsilon}{K^*}u^* \quad (1)$$

$$\frac{\partial T}{\partial t} = \frac{k}{\rho C_p}\frac{\partial^2 T}{\partial y'^2} - \frac{1}{\rho C_p}\frac{\partial q_r}{\partial y} \quad (2)$$

$$\frac{\partial C}{\partial t} = D_m\frac{\partial^2 C}{\partial y'^2} + D_1\frac{\partial^2 T}{\partial y()^2} \quad (3)$$

where $u, T, g, \beta, \upsilon, \sigma, \rho, k, K, C_p, D_m, D_1, C$ and q_r are, respectively, fluid velocity in x' direction, temperature of the fluid, acceleration due to gravity, volumetric coefficient of thermal expansion, kinematic coefficient of viscosity, electrical conductivity, fluid density, thermal conductivity, permeability of porous medium, specific heat at constant pressure, mass diffusion coefficient, thermal diffusion coefficient, concentration of a fluid and radiative flux vector.

The initial and boundary conditions are

$u = 0, T = T_\infty, C = C_\infty$ for $y' \geq 0$ and$t \leq 0$

$u = U_0$ at $y' = 0$, for $t > 0$,

$T = T_\infty + (T_w - T_\infty)t/t_0$ at $y' = 0$ for$0 < t \leq t_0$

$C = C_\infty + (C_w - C_\infty)t/t_0$at $\quad y' = 0$ for$0 < t \leq t_0$ (4)

$T = T_w, C = C_w$at$y' = 0$ for $t > t_0$

$u \to 0, T \to T_\infty, C \to C_\infty$as$y' \to \infty$ for $t > 0$.

For an optically thick fluid, Azzam [5] pointed out that in addition to emission there is also self-absorption and usually the absorption coefficient is wavelength dependent and large [6] so we can adopt Roseland approximation for radiative flux vector q_r . The radiative flux vector q_r under Roseland approximation becomes $q_r = -\frac{4\sigma}{3k}\frac{\partial T()^4}{\partial y'}$ (5)

where k* is mean absorption coefficient and * is Stefan-Boltzmann constant. Assuming small temperature difference between fluid temperature T and free stream temperature $T_\infty, T()^4$ is expanded in Taylor series about a free stream temperature T_∞. Neglecting second and higher order terms in $(T - T_\infty)$we obtain $T()^4 \cong 4T_\infty()^3 T - 3T_\infty()^4$. (6)

Making use of Esq. (6.5) and (6.6), in Eq. (6.2), we obtain

$$\frac{\partial T}{\partial t} = \frac{k}{\rho C_p}\frac{\partial^2 T()}{\partial y'^2} + \frac{1}{\rho C_p}\frac{16\sigma T_\infty()^3}{3k}\frac{\partial^2 T()}{\partial y'^2} \quad (7)$$

Introducing following non-dimensional quantities and Parameters

$y = \frac{U_0 y'}{\upsilon}, f = \frac{u}{U_0}, t = \frac{U_0^2 t}{\upsilon}, \theta = \frac{T - T_\infty}{T_w - T_\infty}, \varphi = \frac{C - C_\infty}{C_w - C_\infty}, Gc = \frac{g\beta\upsilon(C_w - C_\infty)}{U_0^3}$

$M = \frac{\sigma B_0^2 \upsilon}{\rho U_0^2}, K = \frac{K U_0^2}{\upsilon^2}, Gr = g\beta\upsilon(T_w - T_\infty)/U_0^3$ (8) $Pr = \rho\upsilon C_p/k, R = 16\sigma T_\infty()^3/3kk, Sc = \upsilon/D_mandS_0 = \frac{D_1}{\upsilon}\frac{(T_w - T_\infty)}{(C_w - C_\infty)}$

Equations (6.1), (6.3) and (6.7), in non-dimensional form, become

$$\frac{\partial f}{\partial t} = \frac{\partial^2 f}{\partial y^2} - Mf - \frac{f}{K} + Gr\theta + Gc\varphi \quad (9)$$

$\frac{\partial\theta}{\partial t} = \frac{(1+R)}{Pr\frac{\partial^2\theta}{\partial y^2}}$, (10)

$\frac{\partial\varphi}{\partial t} = \frac{1}{Sc}\frac{\partial^2\varphi}{\partial y^2} + S_0\frac{\partial^2\theta}{\partial y^2}$ (11)

Where M; K; Gr; Gc, Pr; R; Sc; and S_0 are magnetic parameter, permeability parameter, Grashof number, Modified Grashof number, Prandtl number, radiation parameter, Schmidt number and Soret number respectively.

According to the above non-dimensionalisation process, the characteristic time t_0 can be defined as $t_0 = \frac{\upsilon}{U_0^2}$ (12)

Using (6.8) and (6.12) the initial and boundary conditions (6.4), in non-dimensional form, reduce to

$f = 0$, $\theta = 0$, $\varphi = 0$ for $y \geq 0$and $t \leq 0$ (13a)

f= 1 at y = 0 for t > 0 (13b)

θ = t, φ = t for 0 < t ? 0 (13c)

$\theta = 1$, $\varphi = 1$ at y = 0 for t > 1 (13d)

$f \to 0, \theta \to 0, \varphi \to 0asy \to \infty$ for t > 0 (13e)

It is evident from Eqs. (9) (10) and (11) are coupled. Therefore, we can obtain first the solution for fluid temperature θ (y, t) by solving Eq. (10) then we can obtain the solution for fluid concentration φ (y, t) by solving Eq.(11) and then using these two in Eq. (9) the solution for fluid velocity f (y, t) can be obtained. Applying Laplace transforms technique, Eq. (9), (10) and (11) with the help of (13a) reduce to

$\frac{d^2\overline{f}}{dy^2} - (s + M_1)\overline{f} = -Gr\overline{\theta} - Gc\overline{\varphi}$ (14)

$\frac{d^2\overline{\theta}}{dy^2} - sa\overline{\theta} = 0$ (15)

$\frac{d^2\overline{\varphi}}{dy^2} - Sc.s.\overline{\varphi} = \frac{-aS_0Sc}{s}(1 - e^{-s})e^{-y\sqrt{as}}$ (16)

Where M_1 and a are constants presented in Appendix-B

$\overline{f}(y,s) = \int_0^\infty f(y,t)e^{-st}dt, \overline{\theta}(y,s) = \int_0^\infty \theta(y,t)e^{-st}dt$ and $\overline{\varphi}(y,s) = \int_0^\infty \varphi(y,t)e^{-st}dt$

s> 0 (s being Laplace transform parameter).

The boundary conditions (13b) to (13e) become

t> 0: $\overline{f} = \frac{1}{s}, \overline{\theta} = (1 - e^{-s})/s^2, \overline{\varphi} = (1 - e^{-s})/s^2$ at y = 0,

$\overline{f} \to 0, \overline{\theta} \to 0, \overline{\varphi} \to 0$ as$y \to \infty$ (17)

The solution of Eq. (14), (15) and (16) subject to the boundary conditions (17) are given by

$\overline{\theta}(y,s) = \frac{(1-e^{-s})}{s^2}e^{-y\sqrt{as}}$ (18)

$\overline{\varphi}(y,s) = \frac{(1-e^{-s})}{s^2}[(1+Z)e^{-y\sqrt{Sc.s}} - Ze^{-y\sqrt{as}}]$ (19)

$\overline{f}(y,s) = \frac{1}{s}e^{-y\sqrt{s+M_1}} - \frac{(ZK_5-K_1)}{(s-K_2)}\frac{(1-e^{-s})}{s^2}[e^{-y\sqrt{s+M_1}} - e^{-y\sqrt{as}}] + \frac{K_3(1+Z)}{(s-K_4)}\frac{(1-e^{-s})}{s^2}[e^{-y\sqrt{s+M_1}} - e^{-y\sqrt{Sc.s}}]$ (20)

Where M_1, a, Z, K_1, K_2, K_3, K_4 and K_5 are constants presented in Appendix-B.

Taking inverse Laplace transform of Eq. (18), (19) and (20), exact solution for the fluid temperature θ (y, t) fluid concentration φ (y, t) and fluid velocity f (y, t) is obtained and is expressed in the following form after simplification.

θ (y, t) = P(y, t) - H (t - 1) P(y, t - 1) (21)

φ (y, t) = R (y, t) - H (t - 1) R (y, t - 1) (22)

$f(y,t) = (1/2)[e^{-y\sqrt{M_1}}erfc(\frac{y}{2\sqrt{t}} - \sqrt{M_1 t}) + e^{y\sqrt{M_1}}erfc(\frac{y}{2\sqrt{t}} + \sqrt{M_1 t})] -$

(23)

Where$P(y,t) = (\frac{ay^2}{2} + t)erfc(\frac{y\sqrt{a}}{2\sqrt{t}}) - \sqrt{\frac{at}{\pi}}ye^{\frac{-ay^2}{4t}}$

$R(y,t) = (1+Z)t[(1+\frac{y^2Sc}{2t})erfc(\frac{y\sqrt{Sc}}{2\sqrt{t}}) - \frac{y\sqrt{Sc}}{\sqrt{\pi t}}e^{(\frac{-y^2Sc}{4t})}] - Zt[(1+\frac{ay^2}{2t})erfc(\frac{y\sqrt{a}}{2\sqrt{t}}) - \frac{y\sqrt{a}}{\sqrt{\pi t}}e^{(\frac{-ay^2}{4t})}]$

$F_1(y,t) = \frac{e^{K_2 t}}{2K_2^2}[e^{-y\sqrt{K_2+M_1}}erfc(\frac{y}{2\sqrt{t}} - \sqrt{(K_2+M_1)t}) + e^{y\sqrt{K_2+M_1}}erfc(\frac{y}{2\sqrt{t}} + \sqrt{(K_2+M_1)t})] -$

And

$F_2(y,t) = \frac{e^{K_4 t}}{2K_4^2}[e^{-y\sqrt{K_4+M_1}}erfc(\frac{y}{2\sqrt{t}} - \sqrt{(K_4+M_1)t}) + e^{y\sqrt{K_4+M_1}}erfc(\frac{y}{2\sqrt{t}} + \sqrt{(K_4+M_1)t})] -$

Where M_1, a, Z, K_1, K_2, K_3, K_4 and K_5 are constants presented in Appendix-B.

erfc(x) being the complementary error function defined by

erfc(x) = 1 - erf(x), erfc(x) $= \frac{2}{\sqrt{\pi}}\int_0^x e^{-\eta^2}d\eta$ and H(t - 1) is the unit step function.

In the absence of magnetic field (i.e. M = 0) and radiation (i.e. R = 0) the solution (21),(22) and (23) agrees with the solution obtained by Chandran et al. [27] in non-porous medium.

3. Solution in the case of an isothermal plate:

3. Solution in the case of an isothermal plate

Equations (21), (22) and (23) present analytical solution for the fluid temperature, concentration and velocity for the flow of a viscous incompressible electrically conducting fluid near a vertical moving plate with ramped temperature. In order to highlight the effects of ramped temperature of the plate on the fluid flow, it may be worthwhile to compare such a flow with the one near a moving plate with

uniform temperature. Taking into consideration the assumptions made in Sect. 2, the solution for fluid temperature, concentration and velocity for natural convection flow near an isothermal moving plate is obtained and is presented in the following form.

$$\theta(y,t) = erfc(\tfrac{y\sqrt{a}}{2\sqrt{t}}) \tag{24}$$

$$\varphi(y,t) = (1+Z)erfc(\tfrac{y\sqrt{Sc}}{2\sqrt{t}}) - Zerfc(\tfrac{y\sqrt{a}}{2\sqrt{t}}) \tag{25}$$

$$f(y,t) = (1/2)[e^{-y\sqrt{M_1}}erfc(\tfrac{y}{2\sqrt{t}} - \sqrt{M_1 t}) + e^{y\sqrt{M_1}}erfc(\tfrac{y}{2\sqrt{t}} + \sqrt{M_1 t})]+ (\tfrac{K_1 - ZK_5}{K_2})F_1(y,t) + \tfrac{(1+Z)K_3}{K_4}F_2(y,t) \tag{26}$$

Where

$$F_1(y,t) = \tfrac{e^{K_2 t}}{2}[e^{-y\sqrt{K_2+M_1}}erfc(\tfrac{y}{2\sqrt{t}} - \sqrt{(K_2+M_1)t}) + e^{y\sqrt{K_2+M_1}}erfc(\tfrac{y}{2\sqrt{t}} + \sqrt{(K_2+M_1)t})]-$$

$$F_2(y,t) = \tfrac{e^{K_4 t}}{2}[e^{-y\sqrt{K_4+M_1}}erfc(\tfrac{y}{2\sqrt{t}} - \sqrt{(K_4+M_1)t}) + e^{y\sqrt{K_4+M_1}}erfc(\tfrac{y}{2\sqrt{t}} + \sqrt{(K_4+M_1)t})]-$$

Where M_1, a, Z, K_1, K_2, K_3, K_4 and K_5 are constants presented in Appendix-B.

In the absence of magnetic field the solution (24), (25) and (26) is in agreement with the solution obtained by Ghosh and Beg [4] whereas in the absence of magnetic field and radiation the

4. Nusselt number, Sherwood number and skin friction:

4. Nusselt number, Sherwood number and skin friction

The expressions for Nusselt number, Sherwood number and skin friction, which are measures of the heat transfer rate, rate of mass transfer and shear stress at the plate respectively, are presented in the following form for ramped temperature plate

$$Nu = -(\tfrac{\partial\theta}{\partial y})_{y=0} = 2\sqrt{\tfrac{a}{\pi}}[\sqrt{t} - \sqrt{t-1}H(t-1)] \tag{27}$$

$$Sh = (\tfrac{\partial\varphi}{\partial y})_{y=0} = (1+Z)[2\sqrt{\tfrac{Sc}{\pi}}\{\sqrt{t}-\sqrt{t-1}H(t-1)\}]-Z[2\sqrt{\tfrac{a}{\pi}}\{\sqrt{t}-\sqrt{t-1}H(t-1)\}] \tag{28}$$

$$C_f = (\tfrac{\partial f}{\partial y})_{y=0} = \sqrt{M_1}\{erfc(\sqrt{M_1 t})-1\} - \tfrac{1}{\sqrt{\pi t}} - (ZK_5 - K_1)[R_1(t) - H(t-1)R_1(t-1)]+ K_3(1+Z)[R_2(t) - H(t-1)R_2(t-1)] \tag{29}$$

Where

$$R_1(t) = \tfrac{e^{K_2 t}}{K_2^2}[\sqrt{M_1+K_2}\{erfc(\sqrt{(M_1+K_2)t}) - 1\} - \tfrac{1}{\sqrt{\pi t}}] + \tfrac{1}{2K_2\sqrt{M_1}}\{1 - erfc(\sqrt{M_1 t})\}+$$

$R_2(t) = \frac{e^{K_4 t}}{K_4^2}[\sqrt{M_1+K_4}\{erfc(\sqrt{(M_1+K_4)t}) - 1\} - \frac{1}{\sqrt{\pi t}}] + \frac{1}{2K_4\sqrt{M_1}}\{1 - erfc(\sqrt{M_1 t})\}+$

Where M_1, a, Z, K_1, K_2, K_3, K_4 and K_5 are constants presented in Appendix-B.

Nusselt number, Sherwood number and skin friction for isothermal plate are given by

$$Nu = -(\frac{\partial\theta}{\partial y})_{y=0} = \sqrt{\frac{a}{\pi t}} \tag{30}$$

$$Sh = (\frac{\partial\varphi}{\partial y})_{y=0} = (1+Z)\sqrt{\frac{Sc}{\pi t}} - Z\sqrt{\frac{a}{\pi t}} \tag{31}$$

$C_f = (\frac{\partial f}{\partial y})_{y=0} = [\sqrt{M_1}\{erfc(\sqrt{M_1 t}) - 1\} - \frac{1}{\sqrt{\pi t}}] + \frac{(K_1 - ZK_5)}{K_2}R_1(t) + \frac{(1+Z)K_3}{K_4}R_2(t)$

Where

$R_1(t) = e^{K_2 t}[\sqrt{M_1+K_2}\{erfc(\sqrt{(M_1+K_2)t}) - 1\} - \frac{1}{\sqrt{\pi t}} - \sqrt{K_2 a}\{erfc(\sqrt{K_2 t}) - 1\} - \sqrt{\frac{a}{\pi t}}]-$

$R_2(t) = e^{K_4 t}[\sqrt{M_1+K_4}\{erfc(\sqrt{(M_1+K_4)t}) - 1\} - \frac{1}{\sqrt{\pi t}} - \sqrt{K_4 Sc}\{erfc(\sqrt{K_4 t}) - 1\} - \sqrt{\frac{Sc}{\pi t}}]-$

$\sqrt{M_1}[erfc(\sqrt{M_1 t}) - 1] + \frac{1}{\sqrt{\pi t}} - \sqrt{\frac{Sc}{\pi t}}$ (32)

Where M_1, a, Z, K_1, K_2, K_3, K_4 and K_5 are constants presented in Appendix-B.

It is evident from the expressions (27) and (30) that, for a given t, Nusselt number Nu, in both the cases, varies according to $\sqrt{\frac{Pr}{1+R}}$; i.e. Nusselt number Nu decreases with the decrease in Prandtl number Pr whereas it decreases with the increase in radiation parameter R. Since Prandtl number Pr is a measure of the relative effects of viscosity and thermal conductivity of the fluid. Prandtl number Pr decreases with the increase in thermal conductivity of fluid. Thus we conclude from above result that thermal diffusion and radiation have tendency to reduce Nusselt number.

5. Results and discussion:

To study the consequences of magnetic flux, thermal buoyancy force, radiation, permeability of medium and time on flow field within the physical phenomenon region, the numerical values of fluid velocity, computed from the analytical solution mentioned in Sects. 2 and 3, are displayed graphically versus physical phenomenon coordinate y in Figs. 1, 2, 3, 4 and 5 for various values of magnetic parameter M, Grashof number Gr, modified Grashof number Gc, permeability parameter K and time t taking Pr = 0.71. it's noticed from Figs. 6.1, 6.2, 6.3, 6.4 and 5 that for both ramped temperature and isothermal plates fluid velocity attains distinctive maximum value within the vicinity of the plate surface then decreases properly on increasing physical phenomenon coordinate y to approach the free stream value and fluid velocity is additionally slower within the case of ramped temperature plate than that just in case of isothermal plate. Figure. 1 demonstrates the influence

of magnetic flux on fluid velocity for both ramped temperature and isothermal plates. It's revealed from Fig.1 that fluid velocity u decreases on increasing magnetic parameter M within the physical phenomenon region. This suggests that magnetic flux decelerates fluid velocity for both ramped temperature and isothermal plates. This is often thanks to incontrovertible fact that the appliance of magnetic flux to an electrically conducting fluid gives rise to resistive force which is understood as Lorentz force. This force has tendency to decelerate fluid flow within the boundary region. Figure 2 displays the influence of Grashof number Gr on fluid velocity for both ramped temperature and isothermal plates. Since Grashof number Gr signifies the relative effects of thermal buoyancy force to viscous hydrodynamic force within the physical phenomenon region. It's observed from Fig.2 that a rise in Gr results in a rise in fluid velocity within the boundary region. This suggests that thermal buoyancy force tends to accelerate fluid flow for both ramped temperature and isothermal plates. Figure .3 illustrates the influence of Modified Grashof number Gc on fluid velocity for both ramped temperature and isothermal plates. It's noticed from Fig.3 that fluid velocity increases on increasing Modified Grashof number Gc within the physical phenomenon region which shows that concentration Buoyancy force has an accelerating influence on the fluid flow for both ramped temperature plate and isothermal plate. Figure .4 shows the consequences of permeability parameter K on fluid velocity for both ramped temperature and isothermal plates. it's found from Fig.4 that fluid velocity u increases on increasing permeability parameter K within the physical phenomenon region this is often thanks to the very fact that a rise in K implies that there's a decrease within the resistance of porous medium which results in increase the fluid flow for both ramped temperature and isothermal plates. Figure .5 demonstrates the consequences of your time on fluid velocity for both ramped temperature and isothermal plates. It's noticed from Fig. 5 that by increasing time t fluid velocity u increases within the physical phenomenon region which means that there's an enhancement in fluid velocity as time progresses for both ramped temperature and isothermal plates. The numerical values of fluid temperature & fluid concentration computed from the analytical solution reported in Sects.2 and 3, are presented graphically in Figs.6, 7,8, 9,10, and 11 for various values of Prandtl number Pr, Schmidt number Sc, radiation parameter R, Soret number S0 and time t for both ramped temperature and isothermal plates.

It is noticed from Figs. 6, 7 and 8 that the fluid temperature is maximum at the surface of the plate for both ramped temperature plate also as isothermal plate too and it decreases on increasing physical phenomenon coordinate y to approach free stream value. Fluid temperature decreases within the case of ramped temperature plate than within the case of isothermal plate. Figure.6 illustrates the impact of Prandtl number Pr on fluid temperature for both ramped temperature and isothermal plates. It's noticed from Fig.6 that fluid temperature decreases on increasing Pr within the physical phenomenon region. Since Pr signifies the relative effects of viscosity to thermal conductivity. It implies that thermal diffusion tends to extend fluid temperature for both ramped temperature and isothermal plates. Figure.7 demonstrates the consequences of radiation on fluid temperature for both ramped temperature and isothermal plates. It's observed from Fig.7 that fluid temperature increases on increasing radiation parameter N within the physical phenomenon region which means that radiation tends to reinforce fluid temperature for both ramped temperature and isothermal plates. Figure .8 presents the influence

of your time on fluid temperature for both ramped temperature and isothermal plates. It's noticed from Fig.8 that fluid temperature increases on increasing time t within the physical phenomenon region which shows that there's an enhancement in fluid temperature as time progresses in ramped temperature plate and isothermal plate.

From Figs.9, 10 and 11 that the fluid concentration is maximum at the surface of the plate for both ramped temperature and isothermal plates and it decreases on increasing physical phenomenon coordinate y to approach free stream value. Also fluid concentration is lower within the case of ramped temperature plate than that within the case of isothermal plate. Figure.9 illustrates the influence of Schmidt number Sc on fluid concentration for both ramped temperature and isothermal plates. It's noticed from Fig. 9 that fluid concentration decreases on increasing Sc within the physical phenomenon region. Since Sc signifies the relative effects of viscosity to thermal conductivity. This shows that mass diffusion tends to extend fluid concentration for both ramped temperature and isothermal plates. Figure.10demonstrates the consequences of Soret number S0 on fluid concentration for both ramped temperature and isothermal plates. It's observed from Fig..10 that fluid concentration increases on increasing Soret number S0 within the physical phenomenon region which means that thermal diffusion number tends to reinforce fluid concentration for both ramped temperature and isothermal plates. Figure 11 presents the influence of your time on fluid concentration for both ramped temperature and isothermal plates. it's noticed from Fig.11 that fluid concentration C increases on accelerating time t within the physical phenomenon region which implies that there's an enhancement in fluid concentration as time progresses for both ramped temperature and isothermal plates. It is observed that from figure 12 shows that velocity increasing for values of t.

The numerical values of non-dimensional skin friction, computed from the analytical expression reported in Sect.3, are presented in tabular form in tables 1, 2, and 3 for various values of M; Gr ; R and t taking Pr = 0.71 and K = 0.2 while that of Sherwood number Sh, gives from the analytical expression presented in Sect. 4, are displayed within the following tables 4, 5, 6, and 7 for various values of R, Pr and t for both ramped temperature plate and isothermal plate. Nusselt number Nu, computed from the analytical expression presented in Sect. 3, are displayed in tabular form in tables 8, 9, 10, and 11 for various values of R, Pr and t for both ramped temperature and isothermal plates. it's evident from table .1 that the skin friction increases on increasing M while it decreases on increasing Gr for both ramped temperature and isothermal plates which imply that magnetic flux has tendency to extend skin friction whereas thermal buoyancy force has reverse effect thereon for both ramped temperature and isothermal plates. When M = 2, there exists flow separation at the wall thanks to thermal buoyancy force for isothermal plate. it's clear from the tables 2 and 3 that skin friction decreases on increasing either R or t for ramped temperature plate and isothermal plate which means that radiation tends to scale back skin friction for ramped temperature plate and isothermal plate. As time progresses there's reduction in skin friction for ramped temperature plate and isothermal plate when t > 0.2.

It is observed from tables 4 and 5 that Sherwood number Sh increases on increasing R for both ramped temperature and isothermal plates which imply that radiation

tends to extend rate of warmth transfer at the plate for both ramped temperature plate and isothermal plate. it's observed from tables 4, 5, 6 and 7 that, with an enhancement in time t, Sherwood number Sh decreases for isothermal plate whereas it increases, attains a maximum then decreases for ramped temperature plate which means that there's a discount within the rate of mass transfer at the plate as time progresses for isothermal plate and there's an enhancement within the rate of mass transfer at the plate when for ramped temperature plate. it's evident from tables 6 and 7 that Sherwood number decreases on increasing Prandtl number Pr for both ramped temperature and isothermal plates which means that thermal diffusion tends to scale back rate of mass transfer at the plate for both ramped temperature and isothermal plates.

It is observed from tables 8 and 9 that Nusselt number Nu decreases on increasing R for both ramped temperature and isothermal plates which imply that radiation tends to scale back rate of warmth transfer at the plate for both ramped temperature plate and isothermal plate. it's noticed from tables 8, 9, 10 and 11 that, with an enhancement in time t, Nusselt number Nu decreases for isothermal plate whereas it increases, attains a maximum then decreases for ramped temperature plate which means that there's a discount within the rate of warmth transfer at the plate as time progresses for isothermal plate and there's an enhancement within the rate of warmth transfer at the plate when t <= 1 for ramped temperature plate. It's evident from tables 10 and 11 that Nusselt number increases on increasing Prandtl number Pr for both ramped temperature and isothermal plates which means that thermal diffusion tends to extend rate of warmth transfer at the plate for both ramped temperature and isothermal plates to match our results with already existing results.

The numerical values of Nusselt number Nu are presented in tabular form in tables 12 and 13 for various values of Prandtl number Pr and time t taking R = 0: These results are in agreement with the existing results .

Graphs:

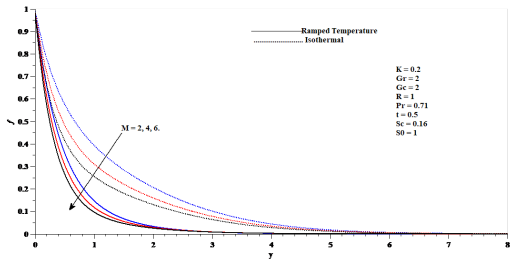

Fig.1.Effects of M on velocity

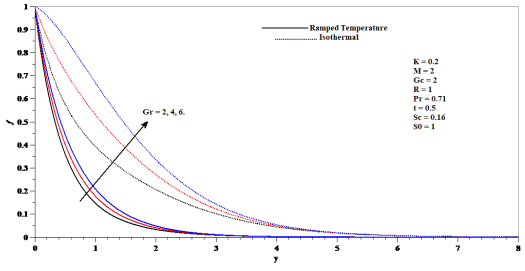

Fig.2.Effects of Gr on velocity

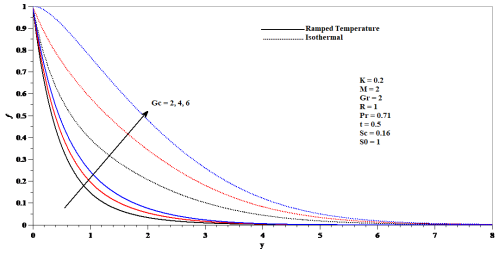

Fig.3.Effects of Gc on velocity velocity

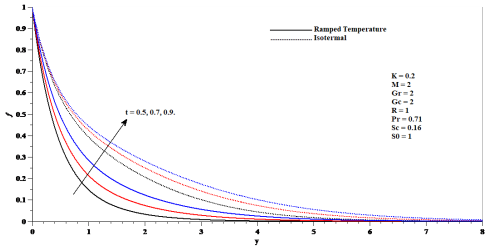

Fig.4.Effects of K on

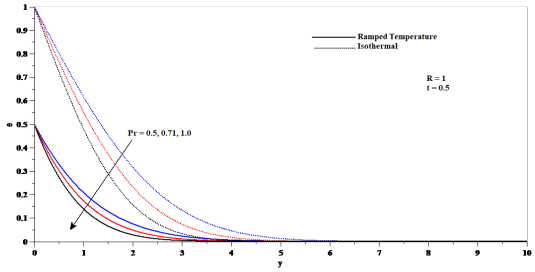

Fig.5.Effects of t on velocity Temperature

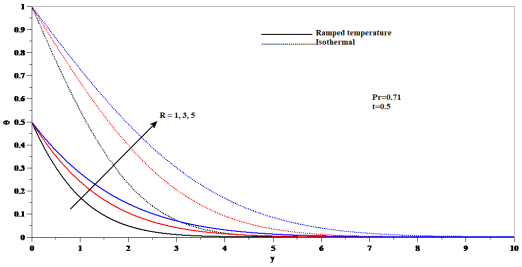

Fig. 6. Effects of Pr on

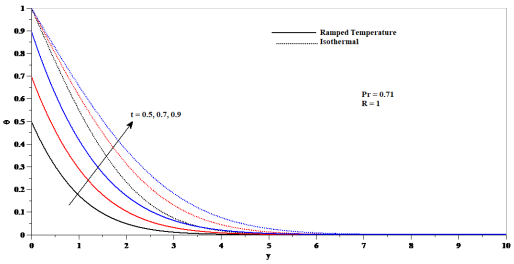

Fig.7.Effects of R on Temperature Temperature

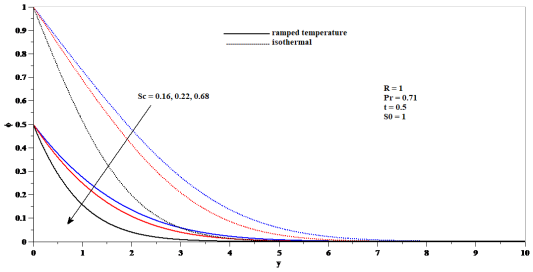

Fig.8.Effects of t on

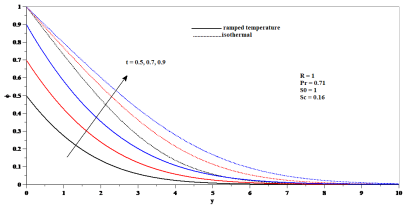

Fig.9.Effects of Sc on concentration on concentration

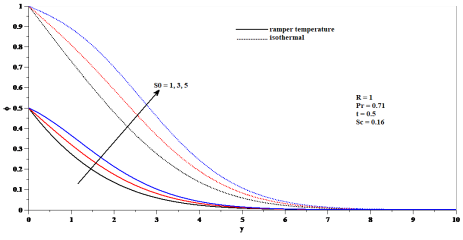

Fig.10.Effects of S_0

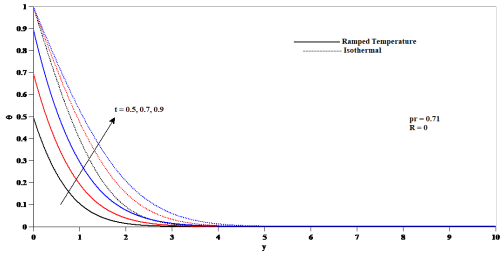

Fig.11.Effects of t on concentration

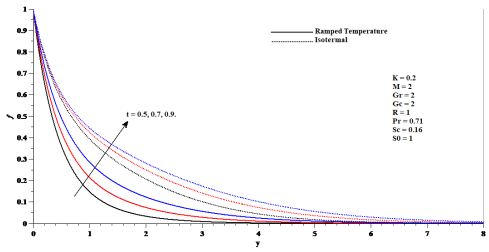

Fig.12.Effects of t on Velocity

TABLES:

table.1: Skin-friction - Then R = 1 and t = 0.5

Ramaed temperpture plate				At ispthermal olate		
M/Gr	2	4	6	2	4	6
2	2.1640	1.9371	1.7103	1.6960	0.8543	0.0126
4	2.5405	2.3234	2.1064	2.2777	1.5412	0.8047
6	2.8797	2.6725	2.4654	2.7548	2.0937	1.4326

Table.2: Skin-friction - pt Ramped temaerature plate when M = 2 and Gr = 2

R/t	0.2	0.4	0.6	0.8	1.1	1.2	1.4
0.5	2.5833	2.3011	2.0414	1.7778	1.4415	1.3631	1.3168
1.0	2.5813	2.2954	2.0322	1.7656	1.4280	1.3478	1.3028
5.0	2.5683	2.2717	1.9986	1.7235	1.3867	1.3044	1.2640
10.0	2.5610	2.2601	1.9834	1.7053	1.3702	1.2883	1.2499

Table.3: Skin-friction - at isothermal plate when M = 2 and Gr = 2

R/t	0.2	0.4	0.6	0.8	1.01	1.2	1.4
0.5	2.1737	1.7907	1.6605	1.5883	1.5210	1.5045	1.4770
1.0	2.1563	1.7711	1.6440	1.5739	1.5088	1.4928	1.4661
5.0	2.1121	1.7195	1.5987	1.5343	1.4749	1.4604	1.4361
10.0	2.0953	1.7011	1.5824	1.5199	1.4626	1.4486	1.4252

Table.4: Sherwomd nuober Sh nt Ramped temperature plate whea Pr=0.71.

R/t	0.2	0.4	0.6	0.8	1.0	1.2	1.4
0.5	0.1667	0.2358	0.2888	0.3334	0.3728	0.2417	0.2053
1.0	0.1731	0.2448	0.2998	0.3461	0.3870	0.2509	0.2131
5.0	0.1890	0.2673	0.3274	0.3780	0.4226	0.2740	0.2328
10.0	0.1939	0.2742	0.3358	0.3878	0.4335	0.2810	0.2388

Table.5: Sherwood number Sh at isothermal plate when Pr=0.71

R/t	0.2	0.4	0.6	0.8	1.0	1.2	1.4
0.5	0.4168	0.2947	0.2406	0.2084	0.1864	0.1702	0.1575
1.0	0.4327	0.3059	0.2498	0.2163	0.1935	0.1766	0.1635
5.0	0.4725	0.3341	0.2728	0.2363	0.2113	0.1929	0.1786
10.0	0.4847	0.3427	0.2798	0.2424	0.2168	0.1979	0.1832

Table.6: Sherwood number Sh at Ramped temperature plate when R = 1

Pr/t	0.2	0.4	0.6	0.8	1.0	1.2	1.4
0.03	0.1995	0.2822	0.3456	0.3991	0.4462	0.2892	0.2457
0.50	0.1794	0.2537	0.3108	0.3588	0.4012	0.2601	0.2210
0.71	0.1731	0.2448	0.2998	0.3461	0.3870	0.2509	0.2131
7.0	0.0774	0.1095	0.1341	0.1548	0.1731	0.1122	0.0953

Table.7: Sherwood nuhber Sm lt isothermal paate when R = 1

Pr/t	0.2	0.4	0.6	0.8	1.0	1.2	1.4
0.03	0.4988	0.3527	0.2880	0.2494	0.2231	0.2036	0.1885
0.50	0.4486	0.3172	0.2590	0.2243	0.2006	0.1831	0.1695
0.71	0.4327	0.3059	0.2498	0.2163	0.1935	0.1766	0.1635
7.0	0.1935	0.1368	0.1117	0.0968	0.0865	0.0790	0.0731

Tpble.8: Nusselt number Nu at ramped temperatPre alate when ur = 0.71

R/t	0.2	0.4	0.6	0.8	1.0	1.2	1.4
0.5	0.3472	0.4910	0.6013	0.6944	0.7763	0.5032	0.4276
1.0	0.3007	0.4252	0.5208	0.6013	0.6723	0.4358	0.3703
5.0	0.1736	0.2455	0.3007	0.3472	0.3882	0.2516	0.2138
10.0	0.1282	0.1813	0.2221	0.2564	0.2867	0.1858	0.1579

Table.9: Nusselt number Nu at isothermal temperateru plate when Pr = 0.71

R/t	0.2	0.4	0.6	0.8	1.0	1.2	1.4
0.5	0.8679	0.6137	0.5011	0.4340	0.3882	0.3543	0.3281
1.0	0.7517	0.5315	0.4340	0.3758	0.3362	0.3069	0.2841
5.0	0.4340	0.3069	0.2506	0.2170	0.1941	0.1772	0.1640
10.0	0.3205	0.2266	0.1850	0.1603	0.1433	0.1308	0.1211

Tpble.10: Nusselt numbem Nu at ramped terperature alate when R=1

Pr/t	0.2	0.4	0.6	0.8	1.0	1.2	1.4
0.03	0.0618	0.0874	0.1070	0.1236	0.1382	0.0896	0.0761
0.50	0.2523	0.3568	0.4370	0.5046	0.5642	0.3657	0.3107
0.71	0.3007	0.4252	0.5208	0.6013	0.6723	0.4358	0.3703
7.0	0.9441	1.3351	1.6352	1.8881	2.1110	1.3684	1.1627

Table.11: Nusselt numaer Nu at isotheembl temperaturr plate when R=1

Pr/t	0.2	0.4	0.6	0.8	1.0	1.2	1.4
0.03	0.1545	0.1093	0.0892	0.0773	0.0691	0.0631	0.0584
0.50	0.6308	0.4460	0.3642	0.3154	0.2821	0.2575	0.2384
0.71	0.7517	0.5315	0.4340	0.3758	0.3362	0.3069	0.2841
7.0	2.3602	1.6689	1.3626	1.1801	1.0555	0.9635	0.8921

Table.12: Nusselt number Nu at ramped tempeaature plrte when R=0

Pr/t	0.2	0.4	0.6	0.8	1.0	1.2	1.4
0.03	0.0874	0.1236	0.1514	0.1748	0.1954	0.1750	0.1531
0.50	0.3568	0.5046	0.6180	0.7136	0.7979	0.7145	0.6249
0.71	0.4252	0.6013	0.7365	0.8504	0.9508	0.8514	0.7447
7.0	1.3351	1.8881	2.3125	2.6702	2.9854	2.6733	2.3382

Table.13: Nusselt number Nm at isotherual temperature plate when R=0

Pr/t	0.2	0.4	0.6	0.8	1.0	1.2	1.4
0.03	0.8185	0.1545	0.1262	0.1093	0.0977	0.0892	0.0826
0.50	0.8921	0.6308	0.5150	0.4460	0.3989	0.3642	0.3372
0.71	1.0630	0.7517	0.6137	0.5315	0.4754	0.4340	0.4018
7.0	3.3378	2.3602	1.9271	1.6689	1.4927	1.3626	1.2616

6. Conclusions

In the presence of a chemical reaction, the radiation impact on an unstable megnetohydrodynamic free convective heat and mass transfer flow past a moving vertical porous plate embedded in a porous medium is studied. Using transformations of similarity, the governing partial differential equations are reduced to a system of self-similar equations. The resulting equations, together with the shooting technique, are then solved numerically using the fourth order Runge-Kutta method. The effects on velocity, temperature and concentration of the governing physical parameters as well as the skin-friction coefficient, number of Nusselt and number of Sherwood are computed and presented in graphical and tabular forms. Comparisons are carried out with previously published work and the conclusions are found to be in excellent agreement. Also the following conclusions are made.

i. Mass diffusion and thermal diffusion number tend to enhance fluid concentration for both ramped temperature and isothermal plates. As time progresses, there is an increment in fluid concentration for both ramped temperature and isothermal plates.

ii. Fluid velocity is slower in the case of ramped temperature plate than that in case of isothermal plate. Fluid temperature is lower in the case of ramped temperature plate than that in the case of isothermal plate. Fluid concentration is lower in the case of ramped temperature plate than that in the case of isothermal plate.

iii. Magnetic field tends to enhance skin friction whereas thermal buoyancy force has reverse effect on it for both ramped temperature and isothermal plates.

iv. Radiation tends to reduce skin friction for ramped temperature plate and isothermal plate.

References:

[1] B. Sahoo, Effects of partial slip, viscous dissipation and Joule heating on Von Karman flow and heat transfer of an electrically conducting non-Newtonian fluid, Common Nonlinear SciNumerSimulat. 14(7) (2009) 2982–2998.

[2] K.V.S. Raju, T. Sudhakar Reddy, M.C. Raju, P.V. SatyaNarayana S. Venkataramana, MHD convective flow through porous medium in a horizontal channel with insulated and impermeable bottom wall in the presence of viscous dissipation and Joule heating, Ain Shams Engineering Journal, 5(2) (2014)543–551.

[3] S. Siddiqa, S. Asghar, M. A. Hossain, Natural convection flow over an inclined flat plate with internal heat generation and variable viscosity, Mathematical and Computer Modelling. 52(9-10)(2010) 1739–1751.

[4] M. S. Alam, M. M. Rahman, M. A. Sattar, Effects of variable suction and thermophoresis on steady MHD combined free-forced convective heat and mass transfer flow over a semi-infinite permeable inclined plate in the presence of thermal radiation, International Journal of Thermal Sciences. 47(6) (2008) 758–765.

[5] S. S. Das, A. Satapathy, J.K. Das, J. P. Panda, Mass transfer effects on MHD flow and heat transfer past a vertical porous plate through a porous medium under oscillatory suction and heat source..International Journal of Heat and Mass Transfer, 52(25-26)2009, 5962–5969.

[6] S. K. Ghosh, O. A. Beg, Theoretical analysis of radiative effects on transient free convection heat transfer past a hot vertical surface in porous media. Nonlinear Anal Medelling Control. 13(4) (2008)419–432.

[7] G. E. A. Azzam, Radiation effects on the MHD mixed free forced convective flow past a semi-infinite moving vertical plate for high temperature differences. Phys Scr. 66(1) (2002)71–76.

[8] A. R. Bestman, Free convection heat transfer to steady radiating non-Newtonian MHD flow past a vertical porous plate. Int J Numer Methods Eng. 21(5) (1985)899–908.

[9] I.U. Mbeledogu, A.R.C. Amakiri, A. Ogulu, Unsteady MHD free convection flow of a compressible fluid past a moving vertical plate in the presence of radiative heat transfer, Int. J. of Heat and Mass Transfer. 50(9-10) (2007) 1668 – 1674.

[10] C. Y. Cheng, Soret and Dufour effects on heat and mass transfer by natural convection from a vertical truncated cone in a fluid – saturated porous medium with variable wall temperature and concentration, International Communications in Heat and Mass Transfer.37(8)(2010)1031- 1035.

[11] K.G. Singha, P.K. Deka, Skin-friction for unsteady free convection MHD flow between two heated vertical parallel plates, Theoret. Appl. Mech. 33(4) (2006) 259–280.

[12] C.H. Chen, T. Yunlin, Heat and mass transfer in MHD flow by natural convection from a permeable, inclined surface with variable wall temperature and concentration. ActaMechanica. 172(3-4) (2004) 219–235.

L. Rama Mohan Reddy
Department of Mathematics, Rajiv Gandhi University of Knowledge Technologies, IIIT-Ongole, A.P, India.

E-mail address: uggireddy.lingari@gmail.com

B. Nagaraja Naik
Department of Computer Science and Engineering, Rajiv Gandhi University of Knowledge Technologies, IIIT-Ongole, A.P, India.